

## The Mechanism of Oxidative Stress Stabilization of the Thromboxane Receptor in COS-7 Cells\*

Received for publication, June 25, 2003, and in revised form, October 16, 2003  
Published, JBC Papers in Press, October 28, 2003, DOI 10.1074/jbc.M306761200

François Valentin<sup>‡§</sup>, Mark C. Field<sup>‡§¶</sup>, and John R. Tippins<sup>‡¶</sup>

From the <sup>‡</sup>Department of Biological Sciences and the <sup>§</sup>Wellcome Trust Laboratories for Molecular Parasitology, Imperial College, Exhibition Road, London SW7 2AZ, United Kingdom

**The 8-iso-prostaglandin  $F_{2\alpha}$ , a prostanoid produced *in vivo* by cyclooxygenase-independent free-radical-catalyzed lipid peroxidation, acts as a partial agonist on the thromboxane receptor (TXA<sub>2</sub>R) and is a potent vasoconstrictor in the oxidatively stressed isolated perfused rat heart. We hypothesized that the response in the isolated heart may be due to augmentation of TXA<sub>2</sub>R density, which may be initiated by the presence of oxidative radicals. Previous studies have shown that TXA<sub>2</sub>R density is increased during atherosclerosis on both the medial and intimal smooth muscle layers in human coronary arteries. Here we describe the effect of oxidative stress on TXA<sub>2</sub>R. The thromboxane A<sub>2</sub> receptor  $\beta$  isoform (TXA<sub>2</sub>R $\beta$ ) was transiently expressed in COS-7 cells. Immunofluorescence suggested that the presence of H<sub>2</sub>O<sub>2</sub> increased translocation of TXA<sub>2</sub>R $\beta$  from the endoplasmic reticulum (ER) to the Golgi complex. H<sub>2</sub>O<sub>2</sub> treatment also increased binding of a TXA<sub>2</sub>R antagonist (<sup>3</sup>H]SQ29548) to membranes. Degradation kinetics of TXA<sub>2</sub>R $\beta$  following cycloheximide treatment, a protein synthesis inhibitor, suggested not only that TXA<sub>2</sub>R $\beta$  is a short-lived protein predominantly localized to the ER but also that TXA<sub>2</sub>R $\beta$  degradation is modulated in the presence of H<sub>2</sub>O<sub>2</sub>. Our results indicate that oxidative stress induces maturation and stabilization of the TXA<sub>2</sub>R $\beta$  protein probably by intracellular translocation. Importantly, these observations also suggest that TXA<sub>2</sub>R $\beta$  levels are modulated by ER-associated degradation and controlled by the efficiency of transport to post-ER compartments. Stabilization of the TXA<sub>2</sub>R $\beta$  by translocation from a degradative compartment, *i.e.* the ER, can account for the augmentation of receptor density observed *in vivo*.**

Thromboxane A<sub>2</sub> (TXA<sub>2</sub>)<sup>1</sup> is an unstable arachidonate metabolite, implicated as a mediator in diseases such as myocardial infarction, stroke, and bronchial asthma (1). Binding of TXA<sub>2</sub> to its receptor, a polytopic membrane-spanning protein, induces vasoconstriction and platelet aggregation, as well as

mitogenesis and hypertrophy of vascular smooth muscle cells (2). Two TXA<sub>2</sub> receptor (TXA<sub>2</sub>R) isoforms have been identified, TXA<sub>2</sub>R $\alpha$  (343 amino acids), which is mainly located in the placenta, and TXA<sub>2</sub>R $\beta$  (407 amino acids), located in the endothelium; these isoforms are generated by the alternative splicing of a single gene (3, 4). The TXA<sub>2</sub>R is part of the G protein-coupled receptor superfamily, and evidence suggests that TXA<sub>2</sub>-induced production of second messenger inositol polyphosphates results from the activation of the G<sub>q11</sub> family of heterotrimeric G proteins (5).

Isoprostanes are formed by free radical attack on membrane phospholipids during oxidative stress (6). They are found in increased concentration in patients with coronary heart disease and are potent vasoconstrictors (7). We have shown that one of these, the 8-iso-prostaglandin F<sub>2 $\alpha$</sub> , is a potent coronary vasoconstrictor, and its effect is exerted via partial agonist action on the TXA<sub>2</sub>R (8). This mechanism of action on TXA<sub>2</sub>R, in vascular smooth muscle and in platelets, has been confirmed in a TXA<sub>2</sub>R knock-out mouse (9). Our data suggested that a critical determinant of the intrinsic activity of the isoprostane is the TXA<sub>2</sub>R reserve, and this has subsequently been supported by another study (10). We have shown that, in the normal rat heart perfused at constant pressure in the Langendorff mode, 8-iso-prostaglandin F<sub>2 $\alpha$</sub>  had no effect, even though U46619, a TXA<sub>2</sub>R agonist, produced a pronounced vasoconstriction. However, after an oxidative stress induced by 30 min of low flow and reperfusion or by a superoxide-generating system (*i.e.* xanthine and xanthine oxidase), 8-iso-prostaglandin F<sub>2 $\alpha$</sub>  became a potent vasoconstrictor, whereas the response to U46619 was unchanged (11). Responses to both agonists were inhibited by the TXA<sub>2</sub>R antagonist SQ29548, suggesting that they act upon the same receptor.

The rapidity of the change in response suggests that this is unlikely to be due to alterations in gene expression and could be explained in several ways including loss of NO-mediated physiological antagonism (12), changes in the second messenger systems that transduce the response to isoprostane, or an increase in receptor reserve. Evidence for this last possibility has been gained from clinical studies; platelet TXA<sub>2</sub>R expression is increased in patients in acute myocardial infarction (13), and in human coronary arteries TXA<sub>2</sub>R density is augmented during cardiovascular disease (14, 15). One of the possible mechanisms for oxidative stress to increase the TXA<sub>2</sub>R reserve could be the relocation of an inactive pool of receptor; in hypoxic or ischemic hearts, oxidative stress may induce the translocation of glucose transporters GLUT 1 and GLUT 4 (16). Alternatively, stabilization of the protein could account for activation; in melanoma cells, dihydroxyphenylalanine induces the transition of misfolded wild type tyrosinase to the native and functional form, which is competent to exit the ER (17). We hypothesized that oxidative stress could act on the TXA<sub>2</sub>R folding, as dihydroxyphenylalanine on tyrosinase, through the

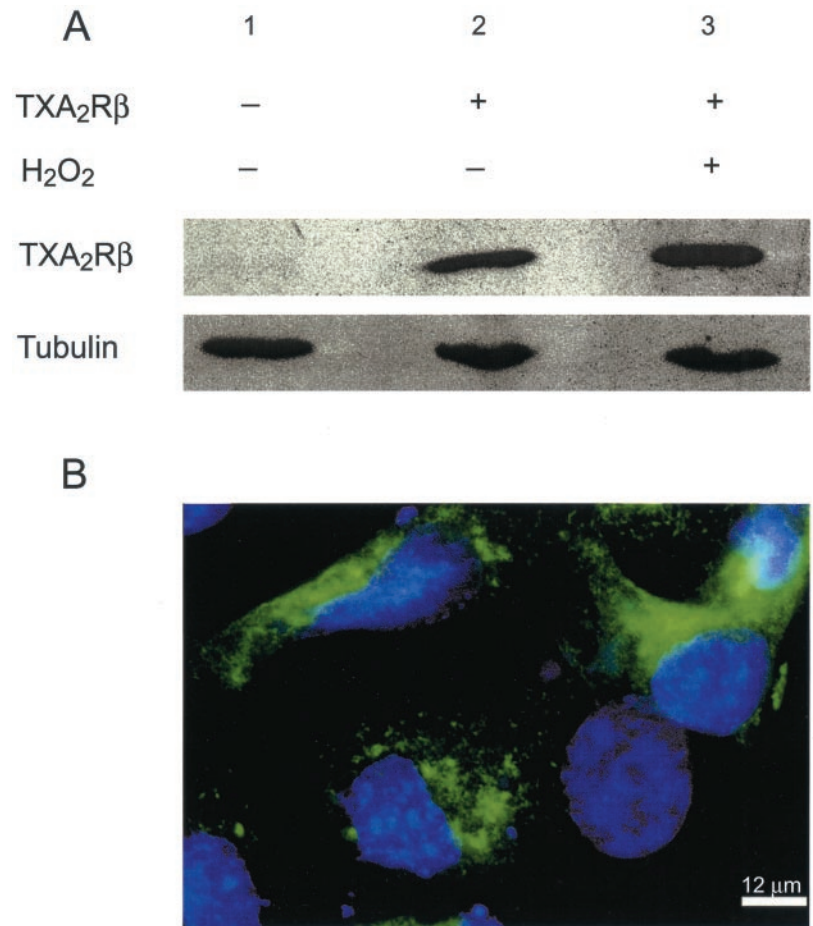
\* This work was supported by British Heart Foundation Grant PG/2000119 (to J. R. T. and M. C. F.). The costs of publication of this article were defrayed in part by the payment of page charges. This article must therefore be hereby marked "advertisement" in accordance with 18 U.S.C. Section 1734 solely to indicate this fact.

¶ To whom correspondence may be addressed. Tel./Fax: 44-020-7594-5277; E-mail: m.field@imperial.ac.uk.

§ To whom correspondence may be addressed. Tel.: 44-020-7594-5216; Fax: 44-020-7594-5300; E-mail: j.tippins@imperial.ac.uk.

<sup>1</sup> The abbreviations used are: TXA<sub>2</sub>, thromboxane A<sub>2</sub>; TXA<sub>2</sub>R $\beta$ , thromboxane A<sub>2</sub> receptor  $\beta$  isoform; ER, endoplasmic reticulum; BFA, brefeldin A; UPR, unfolded protein response; HCASMc, human coronary artery smooth muscle cells; CHO, Chinese hamster ovary; DAPI, 4',6-diamidino-2-phenylindole; GFP, green fluorescent protein; DTT, dithiothreitol.

**FIG. 1. Localization and expression of TXA<sub>2</sub>R $\beta$  in COS-7 cells.** COS-7 cells were transfected with TXA<sub>2</sub>R $\beta$ -Myc-His, and cell homogenates were analyzed by immunoblotting using anti-Myc antibodies (A). TXA<sub>2</sub>R $\beta$ -Myc-His was detected in the transiently transfected cell lysate (A, lane 2). In contrast, no detectable endogenous TXA<sub>2</sub>R $\beta$ -Myc-His was observed in the nontransfected cell lysate (A, lane 1). An increased TXA<sub>2</sub>R $\beta$ -Myc-His signal was observed in the oxidatively stressed cell lysate (A, lane 3). To ensure that a GFP tag does not interfere with the receptor localization, COS-7 cells were transfected with TXA<sub>2</sub>R $\beta$  wild type and visualized by immunofluorescence microscopy using rabbit antibody against the C terminus (see "Experimental Procedures"). In permeabilized cells, TXA<sub>2</sub>R $\beta$  wild type was distributed throughout the cell, mainly on a reticular network, suggesting an ER localization (B).



unfolded protein response (UPR) mechanism, which is activated under a variety of stress conditions (18). In this present study, we expressed the TXA<sub>2</sub>R $\beta$  in COS-7 cells by transient DNA transfection, and we have investigated the effect of exposure to hydrogen peroxide on the post-translational behavior of the TXA<sub>2</sub>R $\beta$  isoform.

#### EXPERIMENTAL PROCEDURES

**Materials**—Simian kidney (COS-7) cells were obtained from the American Type Culture Collection. Human coronary artery smooth muscle cells (HCASMc) were obtained from CellWorks (Buckingham, UK). The complete control inducible mammalian expression system (pERV3 CHO stable cell line and the pEGSH vector) was purchased from Stratagene (La Jolla, CA). TXA<sub>2</sub>R $\beta$  cDNA was kindly provided by Drs. J. A. Ware and A. W. Ashton (Albert Einstein College of Medicine, New York). Mammalian expression vector pcDNA 3.1/CT-GFP-TOPO, pcDNA 4/CT-Myc-His, Dulbecco's modified Eagle's medium supplemented with glucose (4.5 g/liter), fetal bovine serum, and antibiotic/antimycotic solution were purchased from Invitrogen. 4',6-diamidino-2-phenylindole (DAPI), anti-Golgin-97 mouse monoclonal antibody, Texas Red-conjugated goat anti-mouse IgG, Texas Red-conjugated goat anti-rabbit IgG, Texas Red-conjugated rabbit anti-goat IgG, and Oregon Green-conjugated goat anti-mouse IgG were purchased from Molecular Probes Inc. (Eugene, OR). Anti-calnexin rabbit polyclonal antibody, anti- $\beta$ -COP goat polyclonal antibody, and anti-GRP78 (BiP) rabbit polyclonal antibody were purchased from Santa Cruz Biotechnology Inc. [<sup>3</sup>H]SQ29548 was obtained from PerkinElmer Life Sciences. SQ29548 was obtained from Cayman Chemical Co. (Ann Arbor, MI). DNA Taq polymerase was obtained from Stratagene. The Bradford protein assay kit was from Bio-Rad. Horseradish peroxidase-conjugated goat anti-rabbit or anti-mouse IgG, horseradish peroxidase-conjugated rabbit anti-goat IgG, anti-Myc Cy3, or fluorescein isothiocyanate-conjugated mouse monoclonal antibody, and all of the other chemicals were purchased from Sigma.

**Subcloning of C-terminal GFP and Myc-His-tagged Human TXA<sub>2</sub>R $\beta$  cDNA**—Human TXA<sub>2</sub>R $\beta$  cDNA was amplified by PCR. The oligonucleo-

tides used were 5'-CGGGATCCATGTGGCCCAACGGCAGT-3' and 5'-CGCAGTGATATCCGCTGTAATCCCAG-3' with BamHI and EcoRV sites (underlined). The PCR product was subcloned into pcDNA 3.1/CT-GFP-TOPO or into the pcDNA 4/CT-Myc-His at the BamHI and EcoRV sites. The insertion of the TXA<sub>2</sub>R $\beta$  cDNA was confirmed by DNA sequencing. The human TXA<sub>2</sub>R $\beta$  wild type vector was made by PCR using the following primers: 5'-CGGGATCCATGTGGCCCAACGGCAGT-3' and 5'-GAATTCCTTACGCCTGTAATCC-3' with BamHI and an introduced stop codon (underlined). The PCR product was subcloned into the mammalian expression vector pcDNA 3.1/CT-GFP-TOPO and verified by sequencing.

**Subcloning of C-terminal Myc-His-tagged Human TXA<sub>2</sub>R $\beta$  cDNA into pEGSH Vector**—Human C-terminal Myc-His-tagged human TXA<sub>2</sub>R $\beta$  cDNA was amplified by PCR from the pcDNA 4/CT-Myc-His construct (see above). The oligonucleotides used were 5'-GATATCT-TATGTGGCCCAACGGCAGT-3' and 5'-GATATCCGCTGTAATCCAGCTG-3' with EcoRV sites (underlined). The PCR product was subcloned into pEGSH vector at EcoRV site. DNA sequencing and DNA digestion confirmed the insertion and the orientation of the TXA<sub>2</sub>R $\beta$ -Myc-cDNA.

**Cell Culture and Expression of the GFP and Myc-His-tagged Human TXA<sub>2</sub>R $\beta$** —COS-7 cells were maintained in Dulbecco's modified Eagle's medium supplemented with 10% heat-inactivated fetal bovine serum and antibiotic-antimycotic at 37 °C in a humidified atmosphere of 95% air and 5% CO<sub>2</sub>. pERV3 CHO stable cells line were maintained in presence of G418 (500  $\mu$ g/ml), and HCASMc were maintained in HCASMc basal medium supplemented with HCASMc growth supplement (CellWorks). To create cell lines expressing TXA<sub>2</sub>R $\beta$ , pcDNA 3.1/CT-GFP-TOPO, or pcDNA 4/CT-Myc-His expression vector containing the cDNAs of the wild type TXA<sub>2</sub>R $\beta$ , GFP-tagged TXA<sub>2</sub>R $\beta$  (pCDNA3.1/TXA<sub>2</sub>R $\beta$ -GFP), or Myc-His-tagged TXA<sub>2</sub>R $\beta$  (pCDNA4/TXA<sub>2</sub>R $\beta$ -Myc-His) were transfected into the cells using FuGENE 6 transfection reagent (Roche Applied Science). To obtain the COS-7 stable cells line, COS-7 cells were transfected with pcDNA 4/CT-Myc-His expression vector and maintained in Dulbecco's modified Eagle's medium in the presence of zeocin (600  $\mu$ g/ml) for 8 weeks.

**Antibody Production**—For antibody production, residues 270–369 of

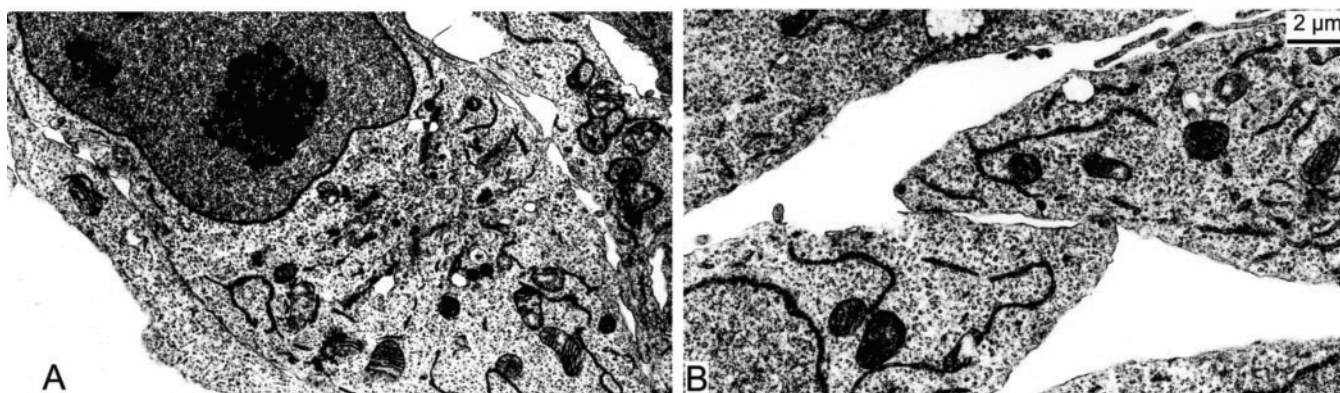
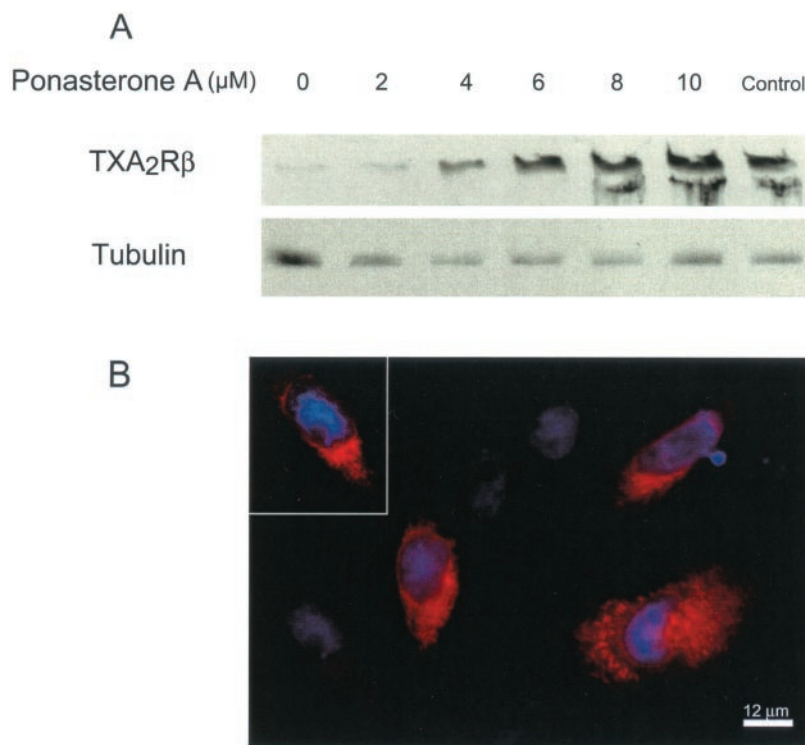


FIG. 2. **Electron microscopy.** To determine whether oxidative stress induces major morphology modifications, COS-7 cells were observed under thin section electron microscopy before (A) and after oxidative stress (B). No gross modification to the morphology of the cells was observed.

FIG. 3. **TXA<sub>2</sub>R $\beta$  expression in pERV3 CHO stable cell line.** pERV3 CHO stable cells were transfected with TXA<sub>2</sub>R $\beta$ -Myc-His (pEGSH vector) and cultured in the presence of different concentrations of the inducer, ponasterone A (0–10  $\mu$ M). The cells were lysed, and the homogenates were analyzed by immunoblotting using anti-Myc antibodies (A). The interaction between the inducer and the ligand-binding domain of the pEGSH vector induced a dose-responsive expression of TXA<sub>2</sub>R $\beta$  (A, first six lanes). Control (homogenate of transiently transfected COS-7 cells) indicated a level of expression similar than the expression in pERV3 CHO cells in presence of 8  $\mu$ M of ponasterone A (A, fifth and seventh lanes). To investigate the intracellular localization of TXA<sub>2</sub>R $\beta$  in pERV3 CHO cells, transiently transfected cells were maintained in presence of ponasterone A (2  $\mu$ M) and visualized by immunofluorescence microscopy (B). The nuclei were stained with DAPI (blue), and TXA<sub>2</sub>R $\beta$  was stained with anti-Myc Cy3 conjugate (red). TXA<sub>2</sub>R $\beta$ -Myc-His was distributed throughout the cell, mainly on a reticular network, suggesting an ER localization. This localization, the same as described above (see Fig. 1) was also obtained at the lowest level of expression (see inset in B with signal augmented by increased gain of the main panel cell indicated by an arrow).



TXA<sub>2</sub>R $\beta$  was amplified using DNA Taq polymerase with the following primers: 5'-CGGGATCCCGAAACCCGCCTGCC-3' and 5'-CGCAGTGAATTCCGCCTGTAATCC-3', cloned into the expression vector pGEX-2TK (Amersham Biosciences) through BamHI and EcoRI sites (underlined), and expressed as a glutathione *S*-transferase fusion protein in *Escherichia coli* DH5 $\alpha$ . Glutathione *S*-transferase fusion protein was inoculated into rabbits with Freund's incomplete adjuvant (Sigma), a procedure repeated four times. Specific antibodies were affinity-purified on antigen immobilized on cyanogen bromide-activated Sepharose 4B (Amersham Biosciences).

**Subcellular Localization of TXA<sub>2</sub>R $\beta$** —COS-7 cells were transfected using pCDNA4/TXA<sub>2</sub>R $\beta$ -Myc-His. At 24 h post-transfection, COS-7 cells were treated with cycloheximide (200  $\mu$ g/ml, 2 h) by adding the drug to the medium, and then the cells were submitted to oxidative stress (H<sub>2</sub>O<sub>2</sub>, 10  $\mu$ M, 40 min). The cells were washed twice in 10 mM triethanolamine, 10 mM acetic acid, 250 mM sucrose, 1 mM EDTA, and 1 mM dithiothreitol, harvested with a rubber policeman in 800  $\mu$ l of buffer containing protease inhibitors (protease inhibitor mixture tablets; Roche Applied Science), and homogenized by 15 passages through a 25-gauge needle on a 1-ml syringe. Nuclei and intact cells were removed by microcentrifugation at 1200  $\times g$  for 5 min at 4  $^{\circ}$ C. The postnuclear supernatant was loaded on preformed Nycodenz gradients prepared exactly as described (19). The postnuclear supernatant was loaded on top of the gradients and centrifuged for 1.5 h at 46,000 rpm in a Beckman L8–55 ultracentrifuge. Equal fractions were collected,

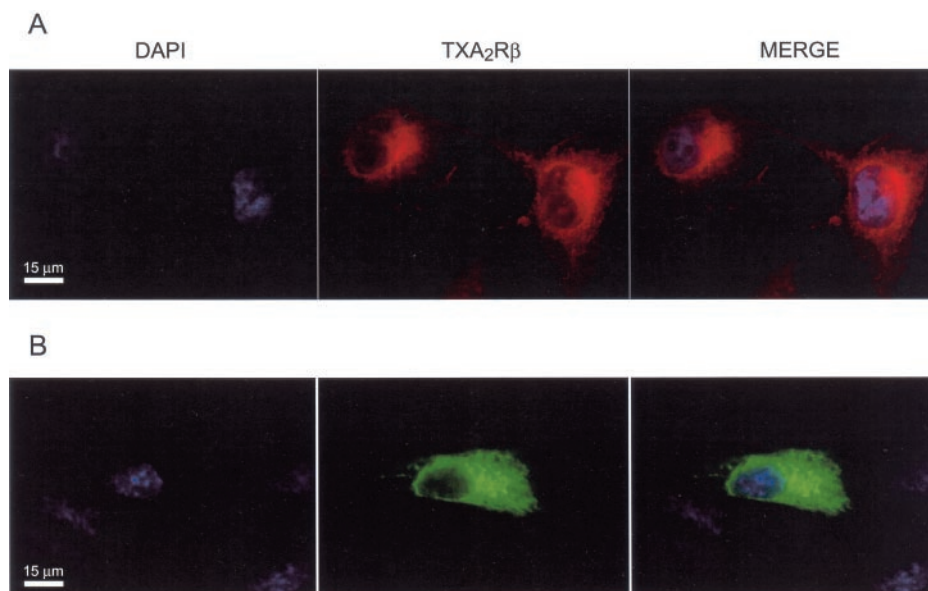
and aliquots of each fraction were subjected to electrophoresis on SDS-PAGE gels. The distribution of TXA<sub>2</sub>R $\beta$ , calnexin (ER marker), and  $\beta$ -COP (intermediate compartment/Golgi complex marker) in the gradients was determined by immunoblotting.

**Immunoblotting**—Protein estimation was performed (Bradford assay), and 20  $\mu$ g of cell lysate protein/lane were electrophoresed on 12% SDS-polyacrylamide gels and blotted onto Hybond-ECL nitrocellulose membrane (Amersham Biosciences) by wet transfer. The filters were blocked in 5% milk, phosphate-buffered saline, and 0.1% Tween 20, probed with primary antibodies (in a 10-ml block) for 1 h, washed four times with phosphate-buffered saline/Tween 20, and then incubated with secondary antibody (diluted 1:5000) in blocking buffer for 1 h and washed. Detection was by chemiluminescence.

**Kinetic Analysis**—COS-7 cells were grown on coverslips and transiently transfected with pCDNA4/TXA<sub>2</sub>R $\beta$ -Myc-His as described above. At 24 h post-transfection, the COS-7 cells were treated with cycloheximide (200  $\mu$ g/ml, 2 h) by adding the drug to the medium, and then cells were submitted to oxidative stress (H<sub>2</sub>O<sub>2</sub>, 10  $\mu$ M, 40 min). The medium was replaced by a new medium containing cycloheximide throughout the experiment. At the indicated time the cells were collected and subjected to electrophoresis on SDS-PAGE gels. Loading control was performed using an anti-tubulin mouse antibody (gift from Keith Gull, Oxford, UK).

**Binding Analysis**—COS-7 cells were grown on coverslips and transiently transfected with pCDNA4/TXA<sub>2</sub>R $\beta$ -Myc-His as described above.

**FIG. 4. TXA<sub>2</sub>R $\beta$  expression in COS-7 stable cell line and in HCASMc.** COS-7 cells were stably transfected with TXA<sub>2</sub>R $\beta$ -Myc-His and visualized by immunofluorescence microscopy (A). The nuclei were stained with DAPI (blue), and TXA<sub>2</sub>R $\beta$  was stained with anti-Myc Cy3 conjugate (red). A perinuclear and reticular network localization was observed, which is consistent with the ER localization described above (Figs. 1 and 3). HCASMc were transiently transfected and visualized by immunofluorescence microscopy (B). The nuclei were stained with DAPI (blue), and TXA<sub>2</sub>R $\beta$  was stained with anti-Myc fluorescein isothiocyanate conjugate (green). Similar ER localization of the receptor was observed (B).



At 24 h post-transfection, the COS-7 cells ( $10^7$ ) were homogenized in 1 ml of binding buffer (25 mM Tris-HCl, pH 7.4, 5 mM CaCl<sub>2</sub>, 10  $\mu$ M indomethacin, 50  $\mu$ g/ml glutathione) using a cell homogenizer. After 5 min of centrifugation at  $1000 \times g$ , the resulting supernatant was centrifuged at  $150,000 \times g$  for 30 min at 4 °C. The pellet corresponding to the membrane fraction was further resuspended in 600  $\mu$ l of binding buffer and homogenized. For the binding assay, 50  $\mu$ g of protein of the membrane fraction was incubated with a TXA<sub>2</sub>R antagonist (<sup>3</sup>H]SQ29548, 30 Ci/mol, 1–100 nM; PerkinElmer Life Sciences) in the presence or absence of 5  $\mu$ M of unlabeled (cold) SQ29548 in a 0.1-ml reaction volume with vigorous shaking at room temperature for 60 min. The reaction was then terminated by adding 1 ml of ice-cold washing buffer (25 mM Tris-HCl, pH 7.4). The unbound ligand was filtered under vacuum through a Whatman GF/C glass filter (Whatman, Clifton, NJ) presoaked with the ice-cold washing buffer. The radioactivity of the TP receptor-bound [<sup>3</sup>H]SQ29548 remaining on the glass filter was counted in 8 ml of scintillation mixture (EN<sup>3</sup>HANCE; PerkinElmer Life Sciences) using a Beckman counter (Fullerton, CA). The  $K_d$  and  $B_{max}$  values (means  $\pm$  S.D.) were compared using Student's unpaired  $t$  test with a significance value of  $p < 0.05$ .

**Immunofluorescence Microscopy**—Cells were fixed for 10 min in phosphate-buffered saline with 3.6% paraformaldehyde and permeabilized for 10 min with phosphate-buffered saline with 0.5% Triton X-100 at room temperature. For the localization of the TXA<sub>2</sub>R $\beta$  wild type, the cells were doubly stained using DAPI (nuclear staining) and polyclonal antibody against the TXA<sub>2</sub>R $\beta$  (described above). The secondary antibody used was Oregon Green-conjugated goat anti-rabbit IgG. For colocalization of TXA<sub>2</sub>R $\beta$ -Myc-His, the cells were stained using DAPI, anti-Myc Cy3-conjugated, and anti-Golgin-97 (*cis*-Golgi marker) monoclonal antibody. The secondary antibody used was Oregon Green-conjugated goat anti-mouse IgG. Immunofluorescence was visualized under a Nikon E600 immunofluorescence microscope equipped with 100 $\times$ /1.3 Plan-Fluor oil immersion objective. The digital images were merged and assembled into figures using Adobe Photoshop (Adobe Systems, Inc.).

**Electron Microscopy**—The cells were fixed in suspension by adding chilled 5% glutaraldehyde and 8% paraformaldehyde in phosphate-buffered saline in a 1:1 ratio to the growth medium. The final dilutions were therefore 2.5% glutaraldehyde and 4% paraformaldehyde. The cells were fixed on ice for 10 min, centrifuged at 3000 rpm for 5 min, and the supernatant carefully replaced with fresh fixative for a further 50 min without disturbing the pellet, rinsed in 0.1 M sodium cacodylate, and post-fixed in 1% osmium tetroxide in the same buffer at room temperature for 1 h. After rinsing in buffer, the cells were then dehydrated in an ethanol series, adding 1% uranyl acetate at the 30% stage, followed by propylene oxide and then embedded in Epon/Araldite 502 and finally polymerized at 60 °C for 48 h. The sections were cut on a Leica Ultracut T ultramicrotome at 70 nm using a diamond knife, contrasted with uranyl acetate and lead citrate, and examined on a Philips CM100 transmission electron microscope.

**Confocal Microscopy**—COS-7 cells were grown on coverslips and transiently transfected with pCDNA3.1/TXA<sub>2</sub>R $\beta$ -GFP. At 24 h post-

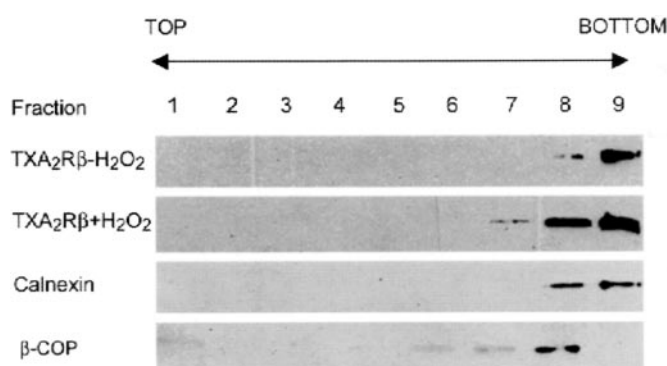


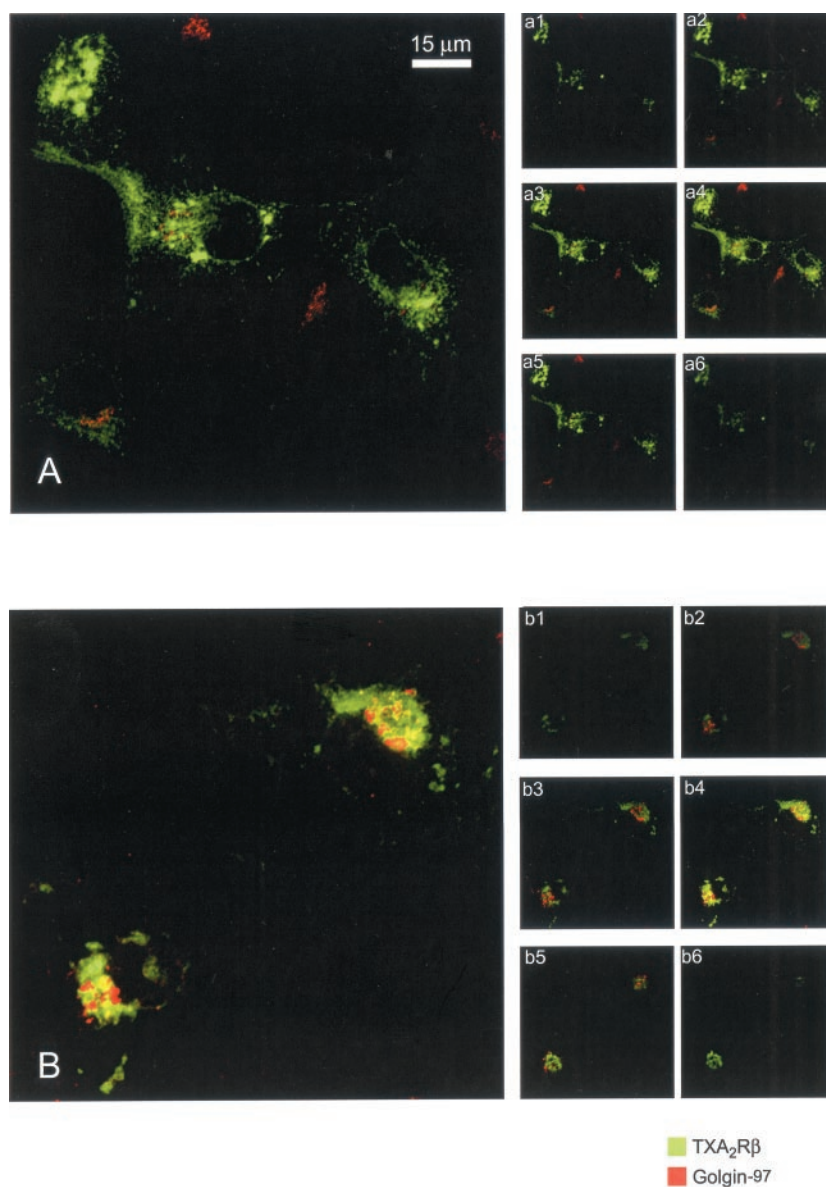
**FIG. 5. Subcellular localization of TXA<sub>2</sub>R $\beta$  on Nycodenz density gradients.** COS-7 cells were transfected with TXA<sub>2</sub>R $\beta$ -Myc-His, and cell homogenates were separated on preformed Nycodenz gradients. The fractions from the gradient were analyzed by immunoblotting using anti-Myc antibodies and other markers as indicated. Marker proteins were calnexin (ER) and  $\beta$ -COP (Golgi complex). In the absence of oxidative stress, a predominantly ER localization for TXA<sub>2</sub>R $\beta$  was observed, whereas in the presence of H<sub>2</sub>O<sub>2</sub>, sedimentation of a proportion of TXA<sub>2</sub>R $\beta$  was shifted to a lighter fraction, co-sedimenting with  $\beta$ -COP. These results suggest that exposure to H<sub>2</sub>O<sub>2</sub> induces a modification of the intracellular localization of the TXA<sub>2</sub>R $\beta$ .

transfection, the cells were incubated 3 h at 37 °C in the presence of 200  $\mu$ g/ml of cycloheximide (control), submitted to oxidative stress, fixed, permeabilized, and stained with the anti-golgin-97 monoclonal antibody and anti-mouse Texas Red-conjugated antibody as described above. The slides were examined using a confocal laser scanning microscope (Axioplan 2 with LSM 510; Carl Zeiss Inc.) equipped with 100 $\times$ /1.4 Plan-APOCHROMAT oil immersion objective. GFP and Texas Red were excited with 488 and 595 nm of krypton-argon lasers, respectively, and individual channels were scanned in series to prevent cross-channel bleed through. Each image represents a single 0.4  $\mu$ m “Z” optical section of GFP-transfected cells.

## RESULTS

**Detection and Localization of TXA<sub>2</sub>R $\beta$  in COS-7 Cells**—COS-7 cells express an endogenous TXA<sub>2</sub>R $\alpha$  (20), suggesting that these cells have the intracellular signaling pathway with which to transduce a response to isoprostane and therefore constitute a relevant model system for this study. Determination of expression of Myc-His-tagged TXA<sub>2</sub>R $\beta$  in COS-7 cells was performed by Western blotting (Fig. 1A). No detectable level of endogenous TXA<sub>2</sub>R $\beta$ -Myc-His was observed in the non-transfected cell lysate (Fig. 1A, lane 1). In contrast, monoclonal antibody was able to detect TXA<sub>2</sub>R $\beta$ -Myc-His in the transiently

**FIG. 6. Confocal microscopy indicates a relocation of TXA<sub>2</sub>Rβ by oxidative stress.** COS-7 cells were transiently transfected with TXA<sub>2</sub>Rβ-GFP (green), and the Golgi complex was visualized with anti-Golgin-97 (*cis*-Golgi marker) and a secondary antibody Texas red (red). At steady state, confocal microscopy analysis showed that TXA<sub>2</sub>Rβ was predominantly localized to the ER (A; *main panel* is the flattened stack, and *small panels* are individual optical sections). In contrast, the addition of H<sub>2</sub>O<sub>2</sub> evoked an intracellular translocation of the TXA<sub>2</sub>Rβ from the ER to the Golgi complex, as demonstrated by co-localization with Golgin-97 (yellow, B).



transfected cell lysate (Fig. 1A, lane 2). Interestingly, the addition of H<sub>2</sub>O<sub>2</sub> (10 μM, 40 min) increased the quantity of TXA<sub>2</sub>Rβ-Myc-His detected in the cell lysate (35 ± 5% increase, *n* = 3; Fig. 1A, lane 3). The observed increase in TXA<sub>2</sub>Rβ-Myc-His quantity present in the cell lysate after H<sub>2</sub>O<sub>2</sub> treatment suggests that the receptor stabilization may occur rapidly after oxidative stress, similarly to that found *in vivo*. Further, TXA<sub>2</sub>Rβ wild type was visualized by immunofluorescence microscopy using rabbit anti-TXA<sub>2</sub>Rβ C-terminal antibody and anti-rabbit fluorescein isothiocyanate conjugate. Immunofluorescence microscopy showed that in permeabilized cells, TXA<sub>2</sub>Rβ wild type was distributed throughout the cell, mainly on a reticular network, suggesting an ER localization (Fig. 1B). To investigate whether oxidative stress could induce some morphology modifications, the cells were observed under electron microscopy before (Fig. 2A) and after oxidative stress (Fig. 2B). No gross modification to the morphology of the cell was observed by thin section electron microscopy, following H<sub>2</sub>O<sub>2</sub> treatment under the conditions used here.

*The Intracellular Localization of TXA<sub>2</sub>Rβ Is Not a Consequence of the Transient Expression*—To investigate whether the intracellular localization of TXA<sub>2</sub>Rβ was a consequence of the expression system, we transfected TXA<sub>2</sub>Rβ into an induc-

ible mammalian expression system. Using the inducible mammalian expression vector (pEGSH vector) containing TXA<sub>2</sub>Rβ, we transiently transfected pERV3 CHO stable cells in the presence of different concentrations of the inducer, ponasterone A (0–10 μM). Western blot analysis revealed that interaction between the inducer and the ligand-binding domain of the pEGSH vector induced a dose-responsive expression of TXA<sub>2</sub>Rβ (Fig. 3A, first six lanes). Control (homogenate of transiently transfected COS-7 cells; Fig. 3A, seventh lane) indicated a similar level of expression to that in pERV3 CHO cells in presence of 8 μM of ponasterone A (Fig. 3A, fifth and seventh lanes). To investigate the intracellular localization of TXA<sub>2</sub>Rβ at low level of expression, transiently transfected cells were maintained in presence of ponasterone A (2 μM) and visualized by immunofluorescence microscopy (Fig. 3B). The nuclei were stained in blue, and TXA<sub>2</sub>Rβ was stained in red. TXA<sub>2</sub>Rβ-Myc-His was distributed throughout the cell, mainly on a reticular network, suggesting an ER localization. This localization, which is consistent with the ER, was obtained even with the minimal detectable level of receptor (see the increased signal gain in Fig. 3B, inset). A similar ER localization was also observed in the stably transfected COS-7 cells line (Fig. 4A) or in transiently transfected HCASMc (Fig. 4B) that endog-

**FIG. 7. Oxidative stress is involved in the stabilization of the TXA<sub>2</sub>Rβ.** COS-7 cells were transfected with TXA<sub>2</sub>Rβ-Myc-His, and cell homogenates were analyzed by immunoblotting using anti-Myc antibodies. Kinetic analysis using cycloheximide was performed to investigate the effect of a H<sub>2</sub>O<sub>2</sub> treatment in the absence of BFA (A) or in the presence of BFA (B) on the half-life of TXA<sub>2</sub>Rβ. The upper panels show representative raw data, with tubulin used as a loading control. The lower panels show quantification of the data normalized at *t* = 0 to 100%. The data suggest that oxidative stress increases the half-life of the TXA<sub>2</sub>Rβ pool (A). This observed stabilization is abolished by BFA (B), suggesting that TXA<sub>2</sub>Rβ stabilization is a consequence of progressing to the Golgi apparatus. The data are representative of three experiments

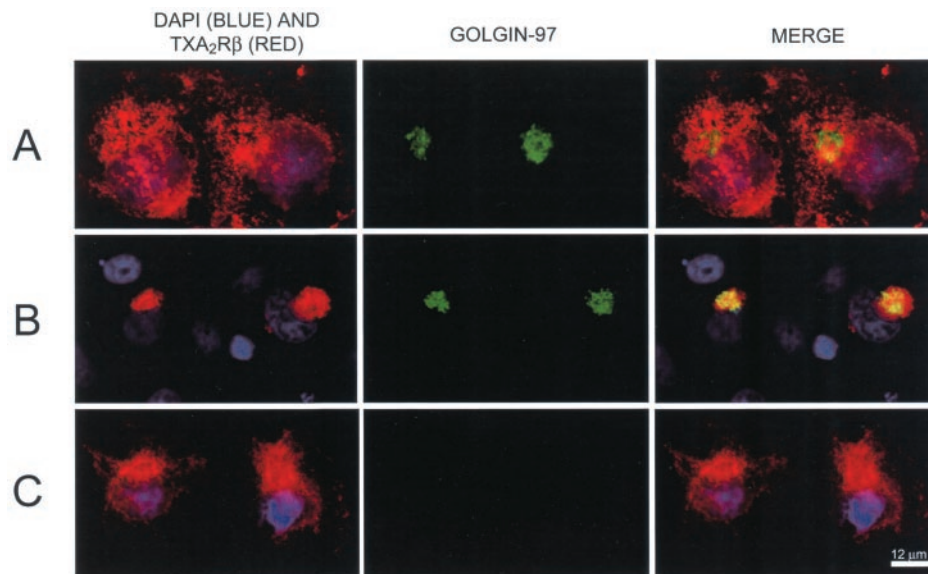
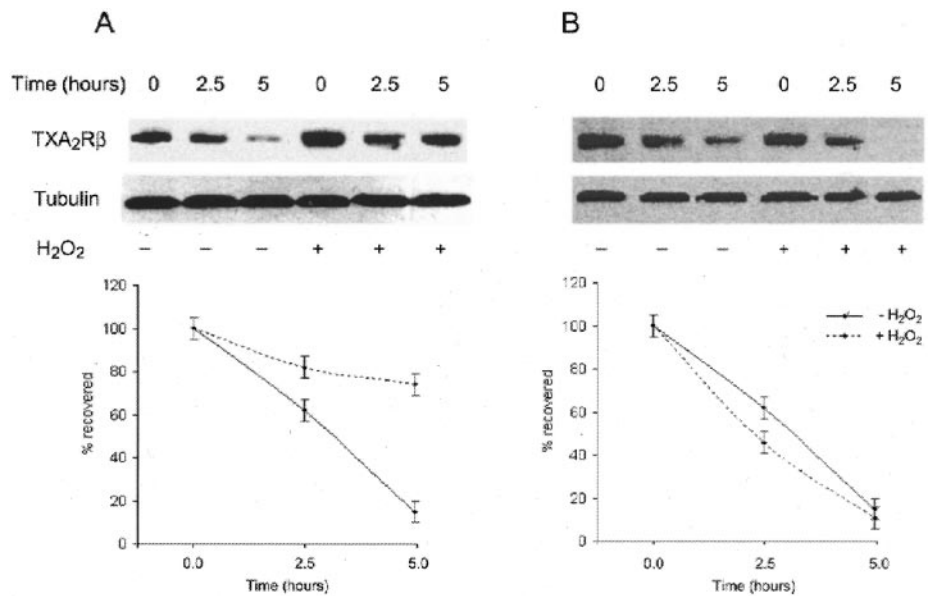


**FIG. 8. Effect of BFA treatment on the TXA<sub>2</sub>Rβ intracellular localization.** COS-7 cells were transiently transfected with TXA<sub>2</sub>Rβ-Myc-His. The nuclei were stained with DAPI (blue), TXA<sub>2</sub>Rβ was stained with anti-Myc Cy3 conjugate (red), and the Golgi complex was stained with anti-Golgin-97 (*cis*-Golgi marker) and an Oregon Green-conjugated secondary antibody (green). Without H<sub>2</sub>O<sub>2</sub> treatment (A), TXA<sub>2</sub>Rβ-Myc-His is detected in structures distributed throughout the cytoplasm with limited co-localization with the *cis*-Golgi complex marker (yellow). By contrast, in the presence of H<sub>2</sub>O<sub>2</sub> treatment (B), TXA<sub>2</sub>Rβ-Myc-His was localized in a very restricted area close to the nucleus showing a co-localization with the *cis*-Golgi complex marker (yellow). Some TXA<sub>2</sub>Rβ-Myc-His was in the ER but below the detection limit. These results confirm that oxidative stress induces a translocation of the receptor to the Golgi complex. BFA treatment on oxidatively stressed cells induces a relocation of the receptor to the ER (C). The disappearance of the Golgi complex staining is due to redistribution of the Golgi complex proteins induced by BFA.

enously express this receptor (21). These data suggest that the ER localization of TXA<sub>2</sub>Rβ is not a consequence of the artificial expression system.

**Oxidative Stress Is Involved in the Intracellular Translocation of TXA<sub>2</sub>Rβ**—To determine more precisely the subcellular localization of TXA<sub>2</sub>Rβ, transiently transfected COS-7 cells were fractionated on nonlinear Nycodenz gradients, using a method previously developed to provide effective separation of ER and Golgi complex proteins (19). As shown in Fig. 5, in the absence of oxidative stress, the main proportion of c-Myc immunoreactivity sedimented to the bottom of the gradient, co-sedimenting with calnexin, a well established ER marker. In contrast, in the presence of H<sub>2</sub>O<sub>2</sub> (10 μm, 40 min), sedimentation of a proportion of TXA<sub>2</sub>Rβ was shifted to a lighter fraction, co-sedimenting with β-COP, a Golgi complex marker (Fig. 5). This observation suggests that upon H<sub>2</sub>O<sub>2</sub> treatment a propor-

tion of the TXA<sub>2</sub>Rβ is translocated to a post-ER compartment.

To confirm this observation, TXA<sub>2</sub>Rβ was localized by confocal fluorescence microscopy. At steady state, confocal microscopy showed that a large proportion of TXA<sub>2</sub>Rβ was localized to the ER (Fig. 6A), and no significant co-localization between TXA<sub>2</sub>Rβ and Golgin-97, a resident Golgi membrane protein, was apparent. In contrast, the addition of H<sub>2</sub>O<sub>2</sub> evoked an intracellular translocation of the TXA<sub>2</sub>Rβ from the ER to the Golgi complex inducing a partial co-localization with Golgin-97 (Fig. 6B, yellow). These results are consistent with the previous observations based on subcellular fractionation suggesting a rapid translocation of the receptor to a post-ER compartment.

**Oxidative Stress Is Involved in the Stabilization of the TXA<sub>2</sub>Rβ**—To determine the role of H<sub>2</sub>O<sub>2</sub> in the biogenesis of TXA<sub>2</sub>Rβ, we used kinetic analysis. At 24 h post-transfection, cycloheximide was used to abolish protein synthesis; TXA<sub>2</sub>Rβ

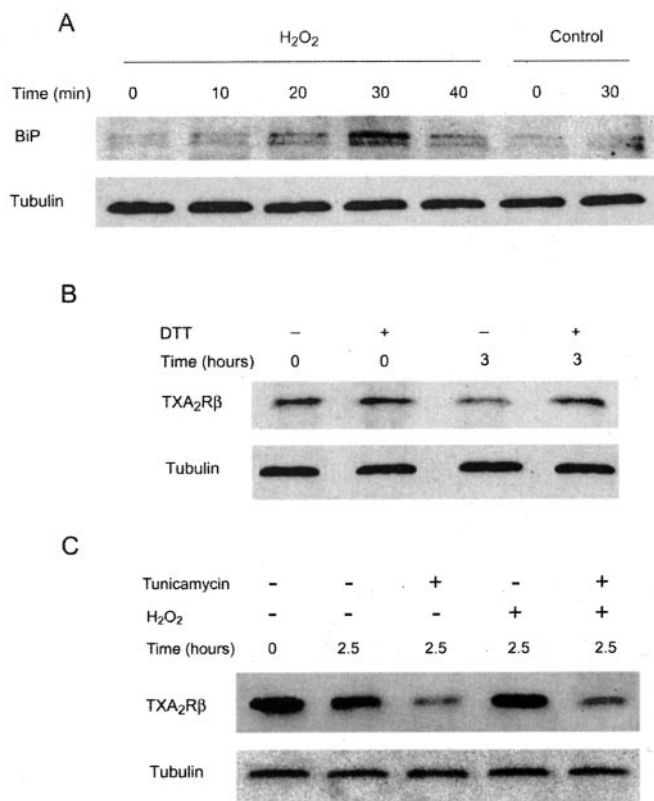


**FIG. 9. Involvement of the UPR in the TXA<sub>2</sub>R $\beta$  stabilization.** COS-7 cells were transfected with TXA<sub>2</sub>R $\beta$ -Myc-His and cell homogenates analyzed by immunoblotting using anti-Myc antibodies. Kinetic analyses of BiP (A), the effect of DTT on cycloheximide-induced TXA<sub>2</sub>R $\beta$  degradation (B), and the effect of tunicamycin on H<sub>2</sub>O<sub>2</sub>-induced TXA<sub>2</sub>R $\beta$  stabilization (C) were performed. The data show that H<sub>2</sub>O<sub>2</sub> induces an up-regulation of BiP expression with a peak reached after 30 min of H<sub>2</sub>O<sub>2</sub> exposure. DTT induced stabilization of TXA<sub>2</sub>R $\beta$ , whereas tunicamycin abolished the H<sub>2</sub>O<sub>2</sub>-induced TXA<sub>2</sub>R $\beta$  stabilization. These results indicate that the UPR is most likely involved in the TXA<sub>2</sub>R $\beta$  stabilization process and that *N*-glycosylation also plays a crucial role.

was chased for different time periods, before Western blot analysis. Fig. 7A shows that in the absence of H<sub>2</sub>O<sub>2</sub>, TXA<sub>2</sub>R $\beta$  is more rapidly degraded than in the presence of H<sub>2</sub>O<sub>2</sub>. After 5 h, TXA<sub>2</sub>R $\beta$  decreased by 80 ± 5% (*n* = 3). In contrast, in the presence of H<sub>2</sub>O<sub>2</sub>, TXA<sub>2</sub>R $\beta$  degradation occurred less rapidly, and only 25 ± 5% of TXA<sub>2</sub>R $\beta$  was degraded after 5 h (*n* = 3), suggesting that oxidative stress is able to mediate TXA<sub>2</sub>R $\beta$  stabilization. This is consistent with the observation in Fig. 1A where H<sub>2</sub>O<sub>2</sub> treatment increased the amount of TXA<sub>2</sub>R $\beta$  detected.

One of the effects of H<sub>2</sub>O<sub>2</sub> on the TXA<sub>2</sub>R $\beta$  is an increase of the proportion of the TXA<sub>2</sub>R $\beta$  in the Golgi complex. We attempted to determine whether the Golgi complex localization had a role in TXA<sub>2</sub>R $\beta$  stabilization. Identical TXA<sub>2</sub>R $\beta$  kinetic experiments to those described above were performed in the presence of brefeldin A (Fig. 7B). BFA treatment abolished the TXA<sub>2</sub>R $\beta$  stabilization induced by the H<sub>2</sub>O<sub>2</sub> (93 ± 5% of degradation after 5 h in presence of BFA *versus* 25 ± 5% in the absence of BFA), without affecting the basal level of TXA<sub>2</sub>R $\beta$  (Fig. 7B). Immunofluorescence microscopy showed that in quiescent cells, TXA<sub>2</sub>R $\beta$  was located mainly in the ER compartment (Fig. 8A). Oxidative stress induced a translocation to the Golgi complex area with an ER staining below the detection limit (Fig. 8B). This translocation is partially abolished by the BFA treatment, which causes disassembly of the Golgi complex (Fig. 8C). In immunofluorescence, essentially no receptors were

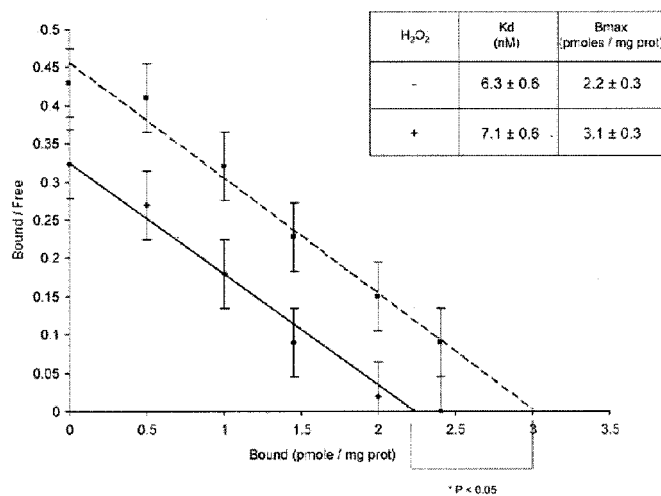


**FIG. 10. Effect of H<sub>2</sub>O<sub>2</sub> treatment on the ligand binding capacity.** COS-7 cells were transiently transfected with TXA<sub>2</sub>R $\beta$ -Myc-His. After homogenization, the membrane fraction was further resuspended in 600  $\mu$ l of binding buffer and homogenized. For the binding assay, 50  $\mu$ g of protein of the membrane fraction was incubated with a TXA<sub>2</sub>R antagonist (<sup>3</sup>H]SQ29548, 30 Ci/mol, 1–100 nM) in the presence or absence of 5  $\mu$ M of unlabeled (cold) SQ29548. Comparison of the [<sup>3</sup>H]SQ29548 binding activities on oxidatively stressed cells (*dotted line*) and nonoxidatively stressed cells (*solid line*) was performed. The data show that the presence of oxidative stress induces an increase of the [<sup>3</sup>H]SQ29548 binding on the membrane fractions (*B*<sub>max</sub> (*B*<sub>max</sub>)) without any effect on the affinity of the receptor (*K*<sub>d</sub> (*K*<sub>d</sub>)).

observed on the plasma membrane, which could be explained by a low receptor density on the plasma membrane of permeabilized cells. Taken together, these results suggest that H<sub>2</sub>O<sub>2</sub> stabilizes TXA<sub>2</sub>R $\beta$  by an intracellular translocation from the ER to the Golgi complex.

**Possible Involvement of the UPR in the TXA<sub>2</sub>R $\beta$  Stabilization**—A potential mechanism for rapid turnover of ER-located TXA<sub>2</sub>R $\beta$  is ER-associated degradation. This pathway is stimulated under numerous stress conditions invoking the UPR. To investigate whether H<sub>2</sub>O<sub>2</sub> exposure could induce the UPR, we evaluated the influence of peroxide on expression of BiP, which is a well characterized UPR gene in mammalian cells (22). A time course of BiP induction upon exposure of cells to 10  $\mu$ M is shown in Fig. 9A. H<sub>2</sub>O<sub>2</sub> induces an up-regulation of BiP with a peak (4–5-fold) of induction at 30 min (Fig. 9A, *fourth* lane). No induction was observed in the absence of oxidative stress (Fig. 9A, *seventh* lane). Exposure to DTT (2 mM, 6 h; Fig. 9B), which is known to be a strong inducer of UPR (23), prevented the TXA<sub>2</sub>R $\beta$  degradation induced by 3 h of cycloheximide treatment (65 ± 5% remaining after 3 h in presence of DTT *versus* 30 ± 5% in the absence of DTT; Fig. 9B, *third* and *fourth* lanes). In contrast, cell treatment with tunicamycin (10  $\mu$ g/ml, 6 h), a further UPR inducer in mammalian cells (23), increased the degradation of TXA<sub>2</sub>R $\beta$  induced by cycloheximide (75 ± 5% remaining after 2.5 h in absence of tunicamycin *versus* 20 ± 5% in presence of tunicamycin; Fig. 9C, *second* and *third* lanes). In addition, the presence of tunicamycin abolished the stabilization of TXA<sub>2</sub>R $\beta$  elicited by H<sub>2</sub>O<sub>2</sub> (75 ± 5% remaining after 2.5 h in absence of tunicamycin *versus* 35 ± 5% in presence of tunicamycin; Fig. 9C, *fourth* and *fifth* lanes). Taken together, these results suggest that UPR might be involved in the TXA<sub>2</sub>R $\beta$  stabilization process and that *N*-glycosylation also seems to play a crucial role in the control of TXA<sub>2</sub>R $\beta$  stability.

**Effect of the H<sub>2</sub>O<sub>2</sub> Treatment on the Ligand Binding Capacity**—A binding assay was performed on an isolated membrane fraction of COS-7 cells using the TXA<sub>2</sub>R antagonist [<sup>3</sup>H]SQ29548. Data show that, in the membrane fraction, H<sub>2</sub>O<sub>2</sub> treatment increased [<sup>3</sup>H]SQ29548-specific binding on the

membrane fraction ( $B_{\max} = 3.1 \pm 0.3$  versus  $2.2 \pm 0.3$  pmol/mg protein,  $p = 0.046$ ,  $n = 3$ ) without any effect on its affinity ( $K_d = 7.1 \pm 0.6$  versus  $6.3 \pm 0.6$  nM,  $n = 3$ ; Fig. 10).

#### DISCUSSION

Most proteins entering the secretory pathway, including TXA<sub>2</sub>Rβ, are folded within the ER following translocation via the Sec61 complex. To support efficient folding, the ER maintains a luminal environment enriched in chaperone proteins, glycosylation enzymes, oxidoreductases, and quality control systems (24). Despite this optimized environment, an inevitable consequence of the large flux of proteins through the ER, plus the complexity of folding, is that rather less than 100% of nascent polypeptides attain the native state, resulting in the production of unfolded proteins. The cells respond to an accumulation of unfolded proteins in the ER by increasing transcription of genes encoding several ER resident proteins. Information on folding status is transmitted from the ER lumen to the nucleus by an intracellular signaling pathway involving the transmembrane kinase Ire1p, called the unfolded protein response (25).

It has been shown that COS-7 cells express an endogenous TXA<sub>2</sub>Rα (20). Transient expression of TXA<sub>2</sub>Rβ in COS-7 cells led to the synthesis of a receptor that was mainly localized to the ER. To investigate whether the artificial expression of TXA<sub>2</sub>Rβ could induce a "mislocalization" of the receptor, TXA<sub>2</sub>Rβ has been expressed in different expression system and/or different cell lines. We always observed an ER localization of TXA<sub>2</sub>Rβ in stably transfected COS-7 cells and when expressed at a low level in a CHO cell line. Similar receptor localization was also observed in HCASMc, another cell line that endogenously expresses TXA<sub>2</sub>Rβ (21). These data indicate that the intracellular localization of TXA<sub>2</sub>Rβ is not due to the system expression but suggest the presence of a significant ER-localized population, which seems to be an intrinsic property of the TXA<sub>2</sub>Rβ. Such a location implicates a possible turnover by the ER-associated degradation system.

Inefficient intracellular processing is not unique to TXA<sub>2</sub>Rβ and has been reported for several other polytopic membrane proteins. For some proteins of this class, e.g. the cystic fibrosis transmembrane conductance regulator, folding is extremely inefficient, with less than 30% of newly synthesized cystic fibrosis transmembrane conductance regulator achieving the native conformation (26). In another example, only 25% of newly synthesized erythropoietin receptor expressed in lymphoid cell lines was processed from the high mannose ER form to the mature plasma membrane form, the remainder being degraded with a half-life of 70 min (27).

We show here that the presence of H<sub>2</sub>O<sub>2</sub> enhanced TXA<sub>2</sub>Rβ translocation from the ER to the Golgi complex, with a concomitant increase in receptor stability. The consequence of such stabilization is an increase of the receptor density in the membrane fraction. Further, additional data indicate that H<sub>2</sub>O<sub>2</sub> treatment induces expression of BiP, a marker for the UPR. Hence, an increase in receptor stability and number is likely the result of more efficient folding caused by induction of the chaperones and other folding activities resident within the ER.

To determine whether stabilization preceded export from the ER or whether it is a consequence of localization within the Golgi apparatus, we tested the effect of BFA, which redistributes cargo proteins of the Golgi complex back to the ER (28) on TXA<sub>2</sub>Rβ degradation. We observed that BFA treatment abolished the TXA<sub>2</sub>Rβ stabilization induced by the H<sub>2</sub>O<sub>2</sub>, suggesting that TXA<sub>2</sub>Rβ stabilization is a consequence of translocation from the ER. It was not particularly surprising that ER-retained TXA<sub>2</sub>Rβ was targeted by the ER-associated degradation and rapidly degraded. Because TXA<sub>2</sub>Rβ is an N-glycosylated

protein (29), the retention of this protein likely involves continued reglycosylation and interaction with the calnexin/glycoprotein glucosyltransferase system (30).

We also have observed that both H<sub>2</sub>O<sub>2</sub> and DTT prevented TXA<sub>2</sub>Rβ degradation. The fact that H<sub>2</sub>O<sub>2</sub> induces BiP expression and mimics the effect on TXA<sub>2</sub>Rβ stabilization induced by DTT, which is known to elicit the UPR (23), suggests that the UPR is involved in the TXA<sub>2</sub>Rβ stabilization. Previous studies using primary dermal fibroblasts identified a rapid effect of the UPR, involving N-linked glycosylation of ER proteins (31). All prostanoid receptors have conserved N-glycosylation sites in the N-terminal domain and one of the extracellular loops. Site-directed mutagenesis studies analyzing the function of glycosylation sites revealed that the requirement of N-glycosylation for correct sorting to the plasma membrane is crucial (32). ER quality control is highly dependent upon covalent attachment of the oligosaccharide Glc<sub>3</sub>Man<sub>9</sub>GlcNAc<sub>2</sub> to specific asparaginyl residues of nascent ER proteins. This requires the synthesis of a lipid-linked oligosaccharide, Glc<sub>3</sub>Man<sub>9</sub>GlcNAc<sub>2</sub>-P-P-dolichol. Tunicamycin is a specific inhibitor of the synthesis of this lipid-linked oligosaccharide and a strong UPR inducer (23). Our results indicate that despite the fact that tunicamycin induces the UPR, it was not able to prevent TXA<sub>2</sub>Rβ degradation and abolished the TXA<sub>2</sub>Rβ stabilization induced by H<sub>2</sub>O<sub>2</sub>. This result supports the model that receptor glycosylation is essential for correct folding and translocation to the plasma membrane as previously shown on cell lines naturally expressing a prostaglandin E1 receptor (33). Because TXA<sub>2</sub>Rβ synthesized in the presence of tunicamycin will not be N-glycosylated, it is likely that correct, efficient folding of the receptor requires interaction with calnexin. Prevention of calnexin interaction will accelerate the rate at which TXA<sub>2</sub>Rβ folding intermediates are rejected by the ER quality control system, ablating the stabilization normally observed with peroxide treatment.

Our results indicate that oxidative stress induces maturation and stabilization of an unstable intracellular TXA<sub>2</sub>Rβ pool, most likely by translocation to the Golgi complex. Importantly, these observations also suggest that TXA<sub>2</sub>Rβ levels are modulated by ER-associated proteolysis and controlled by the efficiency of transport to post-ER compartments. This stabilization of the TXA<sub>2</sub>Rβ by translocation from a degradative compartment may account for the rapid augmentation of receptor density observed *in vivo* and for the potentiation of the 8-iso-prostaglandin F<sub>2α</sub>-induced vasoconstriction during oxidant injury.

*Acknowledgments*—We thank Drs. J. A. Ware and A. W. Ashton for providing cDNA encoding TXA<sub>2</sub>Rβ, David Goulding for electron microscopy technical assistance, Prof. Keith Gull for anti-tubulin antibody, and Dr. Bassam Ali for insightful discussions about many aspects of this work.

#### REFERENCES

1. FitzGerald, G. A., Healy, C., and Daugherty, J. (1987) *Fed. Proc.* **46**, 154–158
2. Narumiya, S., and Sugimoto, Y. (1999) *Physiol. Rev.* **79**, 1193–1226
3. Hirata, M., Hayashi, Y., Ushikubi, F., Yokota, Y., Kageyama, R., Nakanishi, S., and Narumiya, S. (1991) *Nature* **14**, 617–620
4. Raychowdhury, M. K., Yukawa, M., Collins, L. J., McGrail, S. H., Kent, K. C., and Ware, J. A. (1994) *J. Biol. Chem.* **269**, 19256–19261
5. Smrcka, A. V., and Sternweis, P. C. (1993) *J. Biol. Chem.* **268**, 9667–9674
6. Morrow, J. D., Harris, T. M., and Roberts, L. J., II (1990) *Anal. Biochem.* **184**, 1–10
7. Mehrabi, M. R., Ekmekcioglu, C., Tatzber, F., Oguogho, A., Ullrich, R., Morgan, A., Tamaddon, F., Grimm, M., Glogar, H. D., and Sinzinger, H. (1999) *Cardiovasc. Res.* **43**, 492–499
8. Kromer, B. M., and Tippins, J. R. (1996) *Br. J. Pharmacol.* **119**, 1276–1280
9. Audoly, L. P., Rocca, B., Fabre, J. E., Koller, B. H., Thomas, D., Loeb, A. L., Coffman, T. M., and FitzGerald, G. A. (2000) *Circulation* **101**, 2833–2840
10. John, G. W., and Valentin, J. P. (1997) *Br. J. Pharmacol.* **122**, 899–905
11. Kromer, B. M., and Tippins, J. R. (1999) *Br. J. Pharmacol.* **126**, 1171–1174
12. Kamekura, I., Okumura, K., Matsui, H., Murase, K., Mokuno, S., Toki, Y., Nakashima, Y., and Ito, T. (1999) *J. Cardiovasc. Pharmacol.* **33**, 836–842
13. Modesti, P. A., Colella, A., Cecioni, I., Costoli, A., Biagini, D., Migliorini, A., and Neri Serneri, G. G. (1995) *Am. Heart. J.* **129**, 873–879

14. Katugampola, S. D., Kuc, R. E., Maguire, J. J., and Davenport, A. P. (2002) *Clin. Sci.* **103**, 171S-175S.
15. Katugampola, S. D., and Davenport, A. P. (2001) *Br. J. Pharmacol.* **134**, 1385-1392
16. Sun, D., Nguyen, N., DeGrado, T. R., Schwaiger, M., and Brosius, F. C., III (1994) *Circulation* **89**, 793-798
17. Halaban, R., Cheng, E., Svedine, S., Aron, R., and Hebert, D. N. (2001) *J. Biol. Chem.* **276**, 11933-11938
18. Gething, M. J., and Sambrook, J. (1992) *Nature* **355**, 33-45
19. Rickwood, D., Ford, T., and Graham, J. (1982) *Anal. Biochem.* **123**, 23-31
20. Becker, K. P., Ullian, M., and Halushka, P. V. (1998) *Biochim. Biophys. Acta* **27**, 109-114
21. Morinelli, T. A., Zhang, L. M., Newman, W. H., and Meier, K. E. (1994) *J. Biol. Chem.* **269**, 5693-5698
22. Sato, N., Urano, F., Yoon, L. J., Kim S. H., Li, M., Donoviel, D., Bernstein, A., Lee, A. S., Ron, D., Veselits, M. L., Sisodia, S. S., and Thinakaran, G. (2000) *Nat. Cell Biol.* **2**, 863-870
23. Benedetti, C., Fabbri, M., Sitia, R., and Cabibbo, A. (2000) *Biochem. Biophys. Res. Commun.* **278**, 530-536
24. Ellgaard, L., Molinari, M., and Helenius, A. (1999) *Science* **286**, 1882-1888
25. Chapman, R., Sidrauski, C., and Walter P. (1998) *Annu. Rev. Cell Dev. Biol.* **14**, 459-485
26. Kopito, R. R. (1999) *Physiol. Rev.* **79**, S167-173
27. Yoshimura, A., D'Andrea, A. D., and Lodish, H. F. (1990) *Proc. Natl. Acad. Sci. U. S. A.* **11**, 4139-4143
28. Donaldson, J. G., Lippincott-Schwartz, J., Bloom, G. S., Kreis, T. E., and Klausner, R. D. (1990) *J. Cell Biol.* **111**, 2295-2306
29. Chiang, N., and Tai, H. H. (1998) *Arch. Biochem. Biophys.* **352**, 207-213
30. Sousa, M., and Parodi, A. J. (1995) *EMBO J.* **14**, 4196-4203
31. Shang, J., Koerner, C., Freeze, H. H., and Lehrman, M. A. (2002) *Glycobiology* **12**, 307-317
32. Boer, U., Neuschafer-Rube, F., Moller, U., and Puschel, G. P. (2000) *Biochem. J.* **350**, 839-847
33. Yatsunami, K., Fujisawa, J., Hashimoto, H., Kimura, K., Takahashi S., and Ichikawa, A. (1990) *Biochim. Biophys. Acta* **1051**, 94-99